Performance Improvement of a Drop-on-Demand Inkjet Printhead using an Optimization-Based Feedforward Control Method

Amol A. Khalate*,[a], Xavier Bombois[a], Robert Babuška[a], Herman Wijshoff[b], René Waarsing[b]

[a] *Delft Center for Systems and Control, Delft University of Technology, Mekelweg 2, 2628 CD, Delft, The Netherlands.*
[b] *Océ Technologies B.V., P.O. Box 101, 5900 MA Venlo, The Netherlands.*

Abstract

The printing quality delivered by a Drop-on-Demand (DoD) inkjet printhead is limited due to the residual oscillations in the ink channel. The maximal jetting frequency of a DoD inkjet printhead can be increased by quickly damping the residual oscillations and by bringing in this way the ink channel to rest after jetting the ink drop. This paper proposes an optimization-based method to design the input actuation waveform for the piezo actuator in order to improve the damping of the residual oscillations. A discrete-time transfer function derived from the narrow-gap model is used to predict the response of the ink channel under the application of the piezo input. Simulation and experimental results are presented to show the applicability of the proposed method.

Key words: Inkjet printhead, feedforward control, optimization

*Corresponding author:
Tel.: +31 (0)15 27 81362, Fax: +31 (0)15 27 86679,
E-mail address: a.a.khalate@tudelft.nl (Amol A. Khalate)

1. Introduction

The ability of Inkjet technology to deposit materials with diverse chemical and physical properties on a substrate has made it an important technology for both industry and home use. Apart from conventional document printing, the inkjet technology has been successfully applied in the areas of electronics, mechanical engineering, and life sciences. It has been used to manufacture solar panels, PCBs and flat panel displays in the electronics industry. Low cost metal coating and rapid prototyping are popular applications of inkjet printers in mechanical engineering. In the medical field, it has been used for printing DNA structures and making artificial skin by jetting live cells [1]. The success of Inkjet technology in all these application is mainly due to its low operational costs.

A typical drop-on-demand (DoD) inkjet printhead consists of several ink channels in parallel. Each channel is provided with a piezo-actuator, which on application of a standard actuation voltage pulse generates pressure oscillations inside the ink channel. These pressure oscillations push the ink drop out of the nozzle. A detailed description of the droplet jetting process can be found in [2]. The print quality delivered by an inkjet printhead depends on the properties of the jetted drop, i.e., the drop velocity, the jetting direction and the drop volume. To meet the challenging performance requirements posed by new applications, these drop properties have to be tightly controlled.

The performance of the inkjet printhead is limited by two factors. The first one are *residual pressure oscillations*. The actuation pulses are designed to provide an ink drop of a specified volume and velocity under the assump-

tion that the ink channel is in steady state. Once the ink drop is jetted the pressure oscillations inside the ink channel take several micro-seconds to decay. If the next ink drop is jetted before these residual pressure oscillations settle, the resulting drop properties will be different from the ones of the previous drop. This can degrade the printhead performance. The second limiting factor is the *cross-talk*. The drop properties through an ink channel are affected when its neighboring channels are actuated simultaneously. However, the drop velocity variation caused by the cross-talk is much less significant than the one caused by the residual oscillations and will not be addressed in this contribution.

A consequence of the residual oscillations in the ink channel is that the velocity of the drops will only be constant if these drops are jetted at a low frequency. At a high frequency, drops will be jetted before the oscillations in the ink channel have completely disappeared and these residual oscillations will influence the drop velocity. Since a printhead may have to jet drops at different frequencies when printing a bitmap, it is required to be able to jet ink drops with a constant velocity at any rate up to 70kHz. Given this fact, an important characteristic is the so-called DoD curve which represents the ink drop velocity as a function of the jetting frequency (which is also called the DoD frequency). Ideally, the DoD curve must be flat. However, for the reasons given above, this DoD curve is far from flat in practice. Our goal in this paper is to flatten the DoD curve by designing an optimal piezo actuation pulse. Since the residual pressure oscillations in the ink channel are the main reason for which the DoD curve is not flat, our main objective is to reduce these residual oscillations.

Generally, the piezo actuation consists of only one positive trapezoidal pulse which gives good result when only one drop is jetted; we will call this particular actuation pulse the standard pulse. The parameters of the standard pulse are generally tuned by exhaustive studies on a complex numerical model of the inkjet printhead or on an experimental setup [3, 4, 5]. As mentioned earlier, the main drawback of this standard pulse is that it generates residual oscillations. In order to damp the residual oscillations, an additional pulse can be applied after the standard pulse. The actuation pulses used in the literature to damp the residual oscillations can be broadly classified into two categories based on the polarity of the actuation pulse. The first one is an unipolar actuation pulse [6, 7], which consists of the standard pulse to jet an ink droplet and an additional trapezoidal pulse of the same polarity as the standard pulse to damp the residual oscillations. The second category is the bipolar pulse [8, 9, 10], which consists of the standard pulse to jet an ink droplet and the residual oscillations are damped by an additional trapezoidal pulse of opposite polarity of the standard pulse. The advantage of using the bipolar actuation pulse is that the residual oscillations can be damped earlier compared to the unipolar pulse. Conventionally, the parameters of the unipolar and the bipolar pulse are obtained by exhaustive experimental studies, see [7, 8, 9]. The number of experiments needed to design an actuation pulse can be reduced with a wise guess on the parameters of the actuation pulse. It is possible to make an initial guess on the parameters of the actuation pulse as a function of the fundamental period of the channel pressure or the meniscus position [6, 10]. To determine this period, the authors of [2, 6, 10] use an experimental approach. The fundamental

period of the inkjet printhead can be obtained by measuring the ink-channel pressure using a self-sensing mechanism [2, 6] or by measuring the meniscus position using a CCD camera [10]. The meniscus is the ink and air interface in the nozzle. Once the fundamental period is measured, the unipolar pulse and the bipolar pulse can be designed using the parameters recommended in [6] and [10] respectively. However, manual fine tuning of the parameters is needed since the effect of higher-order harmonics is not considered in the design procedure. As opposed to the approaches in [6, 10], we will design the actuation pulse for the DoD inkjet printhead with a systematic model-based approach.

For this purpose, we require a model of the system that we want to control. Here, we consider a discrete-time model $H(q)$ relating the piezo input voltage (i.e., the input) to the velocity of the meniscus (i.e., the output) [11, 2]. We consider this particular model since it is well known that the velocity of the meniscus is a good measure of the pressure in the ink channel [12, 3]. Consequently, reducing the residual oscillations of the meniscus velocity is equivalent to reducing the residual pressure oscillations in the ink channel.

Using this model, we will be able to compute the optimal piezo actuation. Mainly due to the limitations of the driving electronics (see Section 3.1.), the optimal input cannot be computed using a feedback controller, but must be computed off-line based on the model $H(q)$ (feedforward control).

In the literature, we can find other applications of system/control theory to designing off-line the optimal piezo actuation. In [13], the authors propose to inverse $H(q)$ to design the actuation pulse. As the system $H(q)$ is strictly proper and non-minimum phase, it cannot be inverted directly and approx-

imations have to be used. In [2], an iterative learning approach is used to design the optimal pulse off-line. The main drawback of the approach in [2] is that it is not possible to put apriori constraints on the shape of the optimal pulse while such constraints are generally present in practice. Indeed, the driving electronics are generally only able to generate trapezoidal shapes for the piezo actuation input. The approach presented in this paper allows us to deal with such shape constraints. We propose to parameterize the class of piezo input satisfying these shape constraints and to determine the optimal input within this class using an optimization-based approach.

For this purpose, we assume that the possible inputs can be parameterized as $u(k, \theta)$ with θ a parameter vector and k the discrete time index. We then design a template $y_{\text{ref}}(k)$ for the desired meniscus velocity, i.e., a meniscus velocity profile with fast decaying residual oscillations. Based on this template $y_{\text{ref}}(k)$ and the transfer function $H(q)$, an optimal actuation pulse $u(k, \theta_{\text{opt}})$ will be determined as the one minimizing the norm of the tracking error. The proposed method is similar to model predictive control (MPC) [14]. Both these approaches try to reduce the tracking error using an optimization algorithm. The methods differ in the computation of the control input. In the standard MPC algorithm, no constraint on the shape of the control input is imposed.

2. System description and modeling

The DoD inkjet printhead under investigation is made up of two arrays of 128 ink channels each. A cross-sectional view of an ink channel is shown in Figure 1. The ink channel is carved in the channel plate. A filter is placed

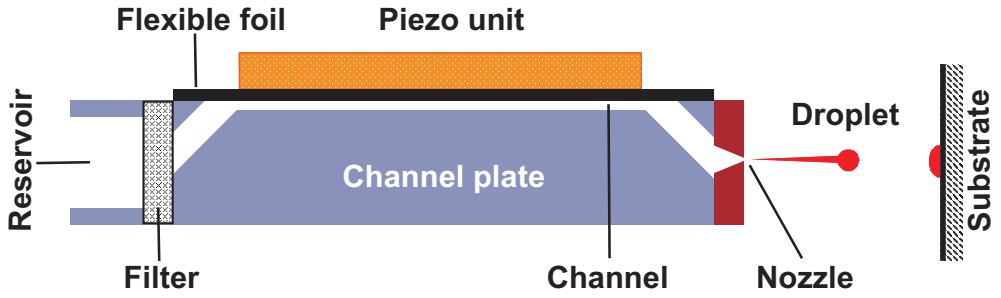

Figure 1: A cross-sectional view of an ink channel.

before the ink channel to remove impurities from the liquid ink. A metallic nozzle-plate with drilled holes, which act as nozzles, is attached at the end of the channel plate. One wall of the ink channel is formed by a flexible foil to which a piezo unit is attached. The piezo unit acts as an actuator and on the application of a voltage, it deforms the wall of the ink channel. The deformation generates pressure waves inside the ink channel and when specific conditions are met, a droplet is jetted [2].

Several analytic and numerical models are available for the inkjet channel dynamics in the literature (for details see [2]). Analytical models are obtained by introducing several assumptions and simplifications. Due to this, the accuracy of analytical models is low compared to numerical models. On the other hand, numerical models are very complex and therefore computationally expensive. For control applications, one prefers a simpler model with a sufficient accuracy. Therefore, we selected the 'narrow-gap model' [15] for control synthesis purposes. The narrow-gap model is an analytical model, which describes the dynamic system from the piezo input voltage u

to the meniscus velocity y. We will use a small droplet DoD inkjet printhead built by Océ Technologies to demonstrate the proposed model-based actuation pulse design method. The viscosity of the ink is $10 \cdot 10^{-3}$ Pa·s and the surface tension of the ink is $28 \cdot 10^{-3}$ Nm^{-1}. The speed of sound in the ink is 1250 ms^{-1}. A detailed derivation of the model for the considered DoD inkjet printhead using the narrow channel theory [15] is given in [11]. In this model, a narrow channel wave equation is used to describe the acoustics inside the ink channel. This wave equation is a simplified form of the Navier-Stokes equation (conservation law for fluids) [11].

In the narrow-gap model, the frequency response $\mathcal{H}(\omega)$ of the system is computed using the sine sweep method. This method consists of solving the wave equation for a sinusoidal input signal $u(t) = |u| \sin(\omega_1 t + \phi_1)$ at some frequency ω_1. Supposing that the corresponding meniscus velocity is given by $y(t) = |y| \sin(\omega_1 t + \phi_2)$, the frequency response of the system at ω_1 is given by:

$$|\mathcal{H}(\omega)|\Big|_{\omega=\omega_1} = \frac{|y|}{|u|} \tag{1a}$$

$$\angle\mathcal{H}(\omega)\Big|_{\omega=\omega_1} = \phi_2 - \phi_1 \tag{1b}$$

By repeating this procedure over a fine frequency grid, we obtain the frequency response given in solid line in Figure 2. It can be seen that the system is non-minimum phase. The narrow-gap model is experimentally validated in [11] by measuring the meniscus velocity on an experimental setup with the help of a laser vibrometer. The empirical frequency function $\mathcal{H}(\omega)$ cannot be used for the optimization leading to the optimal piezo actuation. A transfer function model of the inkjet system is indeed needed for the optimization.

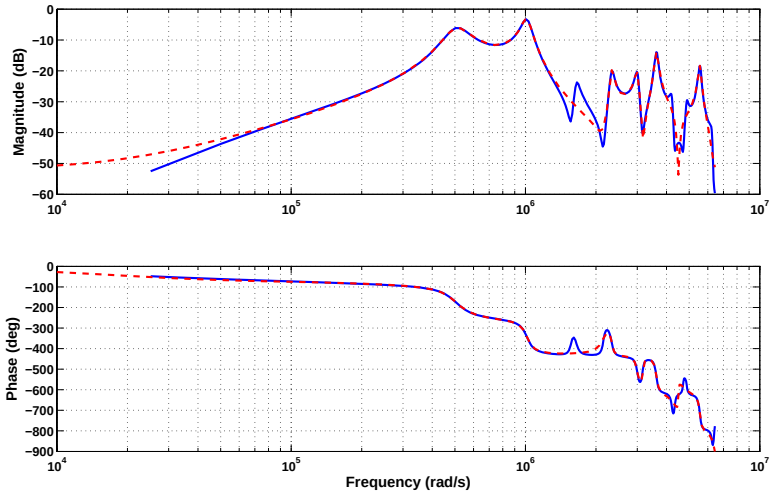

Figure 2: Frequency response of the narrow-gap model $\mathcal{H}(\omega)$ (solid) and frequency response $H(e^{i\omega})$ of the approximated transfer function $H(q)$ (dashed).

Hence, we fit a discrete-time model $H(q)$ to the frequency response obtained from the narrow-gap model. We used the system identification toolbox of MATLAB to approximate the empirical frequency function $\mathcal{H}(\omega)$ by a 16th order discrete-time transfer function $H(q)$. The non-minimum phase behavior present in the frequency response is also captured by the fitted model $H(q)$ shown by the dashed line in Figure 2. This approximated discrete time model will be used for further analysis. Note that the sampling time T_s corresponding to the discrete-time transfer function $H(q)$ was here chosen equal to 0.1μs.

Remarks:

- The narrow-gap model $\mathcal{H}(\omega)$ depends on the printhead geometry and

the properties of the ink material. Hence, the discrete-time transfer function $H(q)$ approximating the frequency response of the narrow-gap model will not be the same for different ink materials and printhead geometries. However, in such situation, we can repeat the procedure above to obtain the discrete-time transfer function $H(q)$ corresponding to the considered situation.

- The narrow-gap model presented in [11] is obtained under the assumption that the acoustic behavior inside the ink-channel is linear. This assumption is valid for the inkjet printheads used in the graphical printing industry. This is thanks to the fact that the meniscus movement with a wide variety of ink materials used in this industry is linear, as these ink materials behave as Newtonian fluids. For several emerging new industrial applications [1], this will not be the case anymore. However, we will see in next section that the proposed method for the actuation pulse design is not limited to linear models. If a nonlinear inkjet system model is available for a non-Newtonian fluid, one can still use the proposed approach to design the actuation pulse in order to damp the residual oscillations.

3. Optimization-based feedforward control design

In this section, we first present the control objectives and foreseen limitations. The proposed optimization-based feedforward control is discussed subsequently.

3.1. Limitations of the control system

The printhead under investigation has very limited control capabilities. The possibility to use feedback control is ruled out due to the following limitations of the actuation system

- No sensor is provided for real-time measurement of the channel pressure or of the meniscus velocity.
- The driving electronics limit the range of the actuation pulses that can be generated in practice. The only possible choice of the actuation pulse is the trapezoidal waveform (Figure 3).
- The sample time required for control computation must be very short due to high drop jetting (DoD) frequency.

In this scenario, the ink channel dynamics can be controlled using a feedforward strategy. The goal is to generate a trapezoidal actuation pulse for the piezo actuator such that the control objectives are met. As mentioned in the introduction, the standard pulse can jet a single ink drop of specified properties, but it is not capable of damping the residual oscillations generated after jetting the ink drop. Therefore, we add a negative trapezoidal pulse in addition to the standard positive trapezoidal pulse in order to damp the residual oscillations, see Figure 3. The actuation signal then consists of a positive trapezoidal pulse (called resonating pulse), which is responsible for jetting the ink drop, followed by the negative trapezoidal pulse which damps the residual oscillations. This pulse is called the quenching pulse. We will see in the sequel that the optimal starting time for this additional negative pulse is approximately equal to the period of the first resonant frequency.

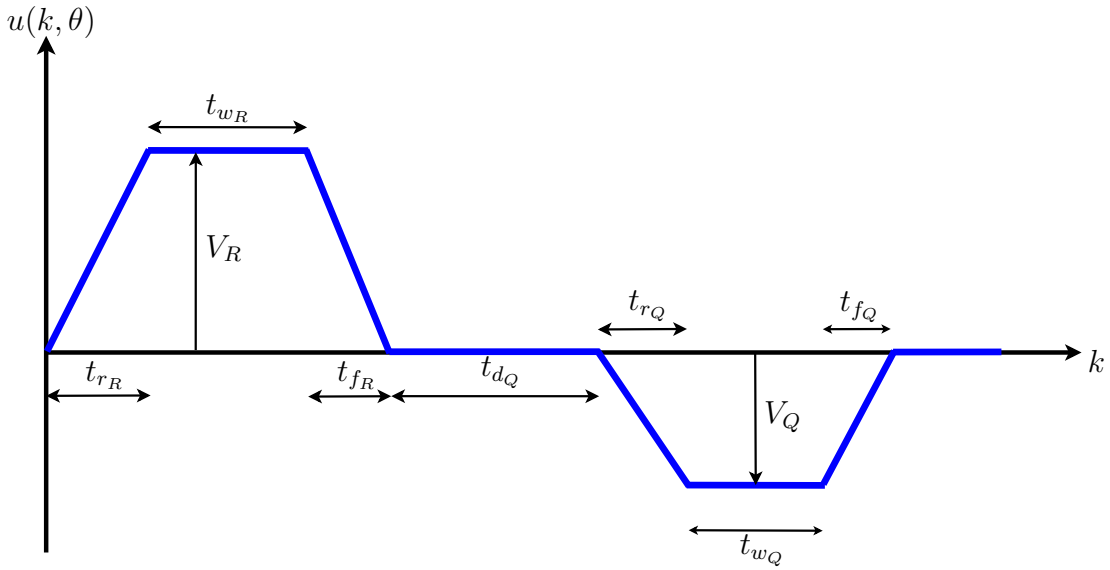

Figure 3: Proposed piezo actuation pulse.

This enables the proposed actuation pulse to jet ink drops at faster DoD frequencies compared to the method proposed in [7, 6]. Now, the actuation pulse can be characterized by the rise time (t_r), the dwell time (t_w), the fall time (t_f) and the amplitude (V) of both the resonating and the quenching pulse. The time interval between the resonating pulse and the quenching pulse is t_{d_Q}. Thus, an actuation pulse $u(k,\theta)$ is defined by the parameter vector $\theta = [t_{r_R}\ t_{w_R}\ t_{f_R}\ V_R\ t_{d_Q}\ t_{r_Q}\ t_{w_Q}\ t_{f_Q}\ V_Q]^T$. Note that in Figure 3, the time parameters (t_r, t_w, t_f, t_{d_Q}) of the actuation pulse are restricted to be equal to an integer multiple of the sampling period T_s. As opposed to the approaches in [8, 9, 10], the optimal parameter vector of the bipolar pulse will be determined using a systematic (optimization-based) approach as shown in the sequel.

3.2. Control Objective

In order to define the optimization problem leading to the optimal parameter vector θ_{opt}, we need a template $y_{\text{ref}}(k)$ for the desired meniscus velocity. In this section we describe the procedure to construct the desired meniscus velocity trajectory $y_{\text{ref}}(k)$ using the transfer function model $H(q)$ and the standard pulse.

For the considered inkjet printhead, the standard pulse is represented in Figure 5 and corresponds to a parameter vector $\theta_{\text{std}} = [1.5\ 2.5\ 1.5\ 25\ 0\ 0\ 0\ 0\ 0]^T$ when using the parametrization of Section 3.1. This standard pulse allows to jet one drop at the desired velocity, but the residual oscillation generated by this standard pulse perturbs the subsequent drops. Such a behavior can be observed in Figure 4 (dashed line) where we represent the response of the model $H(q)$ to the standard pulse. As shown in Figure 4, we can characterize the meniscus velocity response $y(k)$ in two parts. Part A of the response $y(k)$ allows the drop to be jetted at the desired drop velocity. A procedure is described in [12] to predict the properties of the jetted drop using Part A of the meniscus velocity profile. Since we want to jet the ink drop at the desired ink-drop velocity, the desired meniscus velocity $y_{\text{ref}}(k)$ should be the same as $y(k)$ in Part A.

Part B of the response $y(k)$ represents the residual oscillations. This is an undesired behavior, since, the residual oscillations perturb the subsequent drops. Therefore, in Part B, we force the desired meniscus velocity $y_{\text{ref}}(k)$ to zero. This means fast decaying residual oscillations. This template $y_{\text{ref}}(k)$ is represented by the solid line in Figure 4.

Thus, the desired meniscus velocity $y_{\text{ref}}(k)$ is a meniscus velocity profile

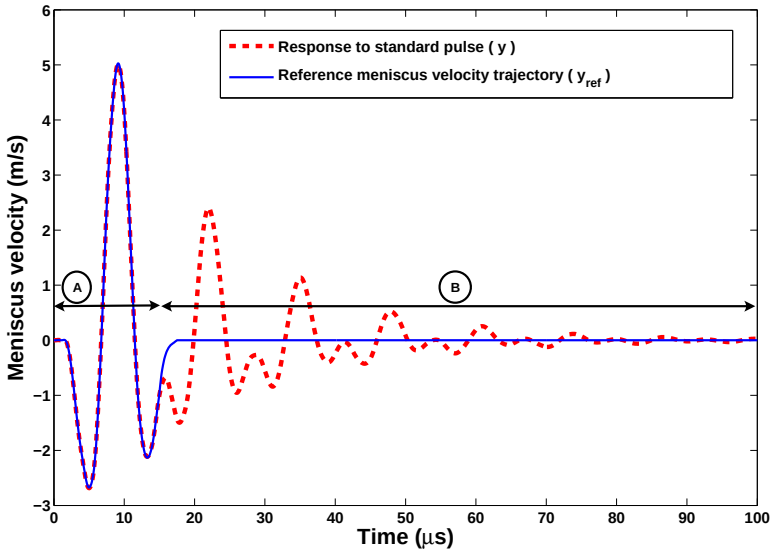

Figure 4: Reference meniscus velocity trajectory.

to jet an ink drop with the desired drop-velocity and fast decaying residual oscillations. If the actuation pulse is designed in such a way that the meniscus velocity $y(k)$ follows the reference trajectory $y_{\text{ref}}(k)$, then the channel will come to rest very quickly after jetting the ink drop. This will create the condition to jet the ink drops at higher jetting frequencies.

3.3. Feedforward control with a trapezoidal pulse

We are now ready to formulate the optimization problem which will lead to the optimal piezo input. The optimal input is the trapezoidal input $u(k, \theta)$ which minimizes the difference between the reference trajectory $y_{\text{ref}}(k)$ and the meniscus velocity $y(k)$. More precisely, we can define the objective func-

tion as the following sum of weighted square errors

$$\mathcal{J}(\theta) = \sum_{k=0}^{N} w(k)\Big(y_{\text{ref}}(k) - y\big(k, u(k,\theta)\big)\Big)^2 \tag{2a}$$

$$= \sum_{k=0}^{N} w(k)\Big(y_{\text{ref}}(k) - H(q)u(k,\theta)\Big)^2 \tag{2b}$$

where $N = \frac{T}{T_s}$, T_s is sampling time, T is chosen equal to $100\,\mu$s, $w(k)$ is a user-defined time-domain weighting, $H(q)$ is the discrete-time model from piezo input to the meniscus velocity, q is here the forward shift operator and $u(k,\theta)$ is the proposed actuation pulse parameterized by the parameter vector θ (see Section 3.1).

Thus, the optimal actuation pulse parameter θ_{opt} is the parameter vector θ solving the following optimization problem

$$\min_{\theta} \mathcal{J}(\theta), \tag{3}$$

subject to

$$\theta_{LB} \leq \theta \leq \theta_{UB}, \tag{4}$$

where, θ_{LB} and θ_{UB} are the vectors containing the lower and the upper bounds on each element of the parameter vector θ.

This is a constrained nonlinear optimization problem and can be solved off-line using standard algorithms. We use the MATLAB function `fmincon`. This function implements a range of optimization techniques. In our experiments we used the default option which is sequential quadratic programming [16, 17].

Remarks:

- The proposed framework is very general and it is not restricted to the meniscus velocity. It is possible to construct the objective function using several other system variables such as the channel pressure signal, the meniscus position, the DoD curve, the flight profile of jetted drops and the velocities of the jetted drops. Moreover, the linear model $H(q)$ for the inkjet system can also be replaced by a nonlinear model if this model allows the computation of the meniscus velocity for all possible piezo inputs. Using nonlinear models will be more accurate when non-Newtonian fluids are jetted.

- Instead of using a model $H(q)$ to generate $y\big(k, u(k,\theta)\big)$ in (2), an actual experimental setup could be used for this purpose. By computing the gradient numerically, we could then perform the optimization of θ. This would be of use when an accurate model is not available. A possible application of this can be the jetting of a non-Newtonian fluid with the inkjet printhead. In this case, a linear model could lead to inaccurate results and obtaining a nonlinear model of the inkjet system may also not be always possible. In such a scenario, one can still obtain the actuation pulse with the proposed method by using the ink channel pressure instead of the meniscus velocity. Indeed, this pressure can be measured by using the piezo unit as an ink-channel pressure sensor (i.e. the self-sensing mechanism [2],[6]). Unfortunately, this approach can not handle severe nonlinearities, see [18].

3.4. Feedforward control with an unconstrained pulse

We have seen that the pulse with constrained shape can be obtained using the nonlinear optimization problem (3)-(4). As mentioned in Section 3.1, this shape constraint is imposed by the driving electronics. From a theoretical point-of-view, it is nevertheless important to verify whether this shape constraint limits the achieved performance to a small or a large extent. In order to perform this verification, a method must be developed to design the pulse minimizing the difference between the actual meniscus velocity and the desired one when no constraints whatsoever are imposed on the shape of this pulse.

One could use for this purpose model predictive control [14]. However, when the control sequence to be computed is long, this method is computationally expensive. We present a simpler and computationally efficient filtering-based approach to generate the unconstrained actuation waveform in order to damp the residual oscillations. For this purpose, we parameterize the to-be-designed actuation pulse as the pulse response of a Finite Impulse Response (FIR) filter $F(q, \beta)$:

$$u(k, \beta) = F(q, \beta)\delta(k) \tag{5}$$

with $F(q, \beta) = \beta_0 + \beta_1\ q^{-1} + ... + \beta_{n_\beta} q^{-n_\beta}$, $\delta(k)$ the unit pulse and $\beta = (\beta_0, ..., \beta_{n_\beta})^T$ a vector containing the coefficients of the FIR filter. When the dimension of β is chosen equal to the desired length of the actuation pulse, this parametrization allows to generate actuation pulses of arbitrary shapes.

For an arbitrary vector β, the response of the ink channel $H(q)$ to the

input $u(k,\beta)$ is given by:

$$y(k,\beta) = H(q)F(q,\beta)\delta(k) = F(q,\beta)H(q)\delta(k) \quad (6a)$$

$$= F(q,\beta)h(k) \quad (6b)$$

where $h(k)$ is the pulse response of the known ink channel dynamics $H(q)$.

The optimal control $u(k,\beta_{\text{opt}})$ is then the one which minimizes the difference between the desired meniscus velocity trajectory $y_{\text{ref}}(k)$ and the achieved meniscus velocity $y(k,\beta)$. Therefore, the optimal parameter vector β_{opt} is the solution of the following optimization problem :

$$\min_{\beta} \sum_{k=0}^{N} w(k)\big(y_{\text{ref}}(k) - F(q,\beta)h(k)\big)^2 \quad (7)$$

Unlike the optimization problem (3) which is nonlinear, the optimization problem (7) leading to the unconstrained actuation pulse is a weighted linear least-squares problem.

Remark:

Determining β can be difficult when the least squares problem (7) is ill-conditioned. In such cases it is advisable to approximately solve the least squares criterion (7) using a truncated Singular Value Decomposition (SVD), to effectively reduce the degrees of freedom in the least squares problem. For more details, see [19].

4. Simulation Results

In the previous section, our control objectives and the related problem of feedforward control design (constrained and not constrained) have been pre-

sented. We will first consider the (realistic) case where the actuation pulse is constrained to have the trapezoidal shape of Figure 3. The nonlinear optimization problem (3)-(4) delivering the optimal trapezoidal pulse is solved by using the `fmincon` function of the MATLAB's optimization toolbox. Recall that the goal is to damp the residual oscillations. Therefore, the weighting $w(k)$ is designed to penalize the tracking error more in Part B of the reference trajectory. The initial guess θ_{init} for the optimal parameter vector needed to solve the nonlinear optimization problem (3)-(4) is chosen as follows

$$\theta_{\text{init}} = [1.5 \quad 2.5 \quad 1.5 \quad 25 \quad 6 \quad 3.6 \quad 1 \quad 1.4 \quad -15]^T.$$

The time parameters (t_r, t_w, t_f, t_{d_Q}) in θ_{init} are chosen using the recommendations in [6] and [10]. The optimal parameter vector θ_{opt} obtained after solving the optimization problem (3)-(4) is given as follows

$$\theta_{\text{opt}} = [2.0 \;\; 2.5 \;\; 1.3 \;\; 22.5 \;\; 7.6 \;\; 1.3 \;\; 0.4 \;\; 4.4 \;\; -13.2]^T.$$

Note that in the parameter vector θ, the time parameters (t_r, t_w, t_f, t_{d_Q}) of the actuation pulse are expressed in μs.

We compare the standard pulse and the optimal actuation pulse in the bottom panel of Figure 5. As expected, the optimal piezo actuation pulse contains two components, the resonating pulse and the quenching pulse. The quenching pulse deflect the piezo actuator in order to damp the residual oscillations. This enables the meniscus velocity to track the reference trajectory very closely and brings the ink channel to rest soon after jetting the ink drop as seen in the top panel of Figure 5 where we compare $y_{\text{opt}}(k) = H(q)u(k, \theta_{\text{opt}})$ to the meniscus velocity corresponding to the standard pulse. As discussed in Section 3.1, the starting time for the quenching

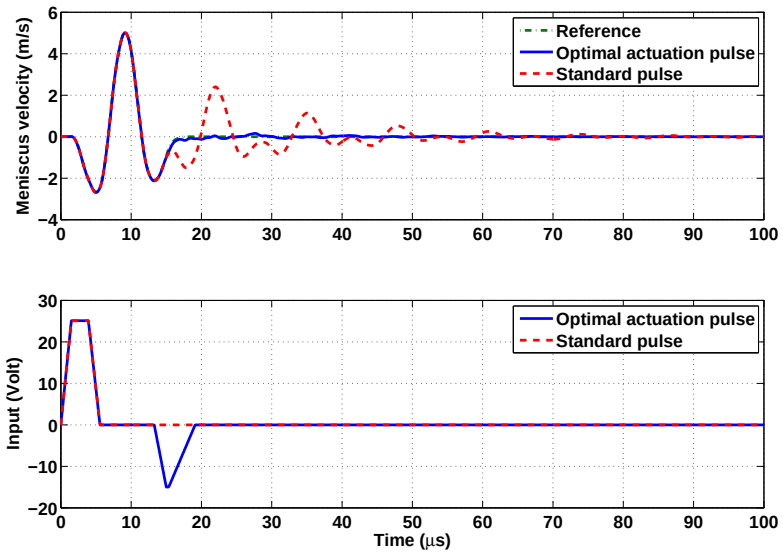

Figure 5: Response of the meniscus velocity to the standard and the optimal actuation pulse.

pulse is approximately 12μs, which is the fundamental period corresponding to the first resonant frequency at 80kHz (see Figure 2). The energy spectral density of the tracking error for the standard pulse and the optimal pulse is shown in Figure 6. It is evident that considerable error reduction is achieved by the optimal pulse at the two dominant resonant frequencies of the inkjet printhead and at low frequency in general.

Given the behavior in Figure 5, ink drops can be jetted with higher frequencies using the optimal actuation pulse. Figure 7 shows the response of the ink channel when ten ink drop are jetted at DoD frequency 38 kHz, i.e., the time interval between the initiation of two actuation pulses is (1/38) ms. In this figure, we compare the behavior when the standard and the optimal

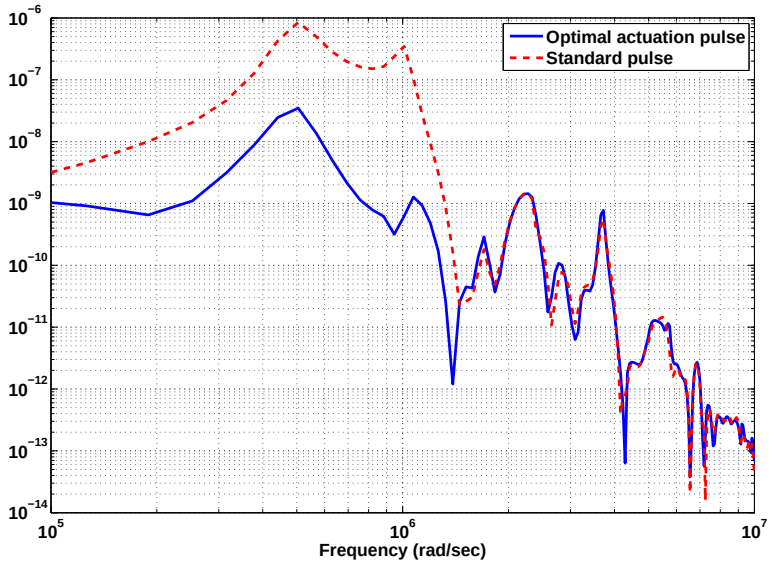

Figure 6: Energy spectral density of the error signal ($y_{\text{ref}} - y$)

pulses are used. The meniscus velocity does not quickly come to rest after jetting the ink drop for the standard actuation pulse. Therefore, the initial conditions differ when applying the subsequent actuation pulses. This causes the velocity-peaks to change for subsequent drops as indeed observed in Figure 7 where they are not equal to $5\,\text{ms}^{-1}$ as in Figure 4. Recall that the velocity peak is a major feature and that a changed velocity-peak will result in drops having different velocities. These short comings are not seen with the optimal piezo actuation pulse. It ensures similar initial conditions before the application of the resonating pulse for each ink drop. The difference in the velocity-peaks for the optimal actuation pulse are almost negligible. This will result into ink drops having almost the same velocity.

We have done similar experiments at different DoD frequencies to analyze

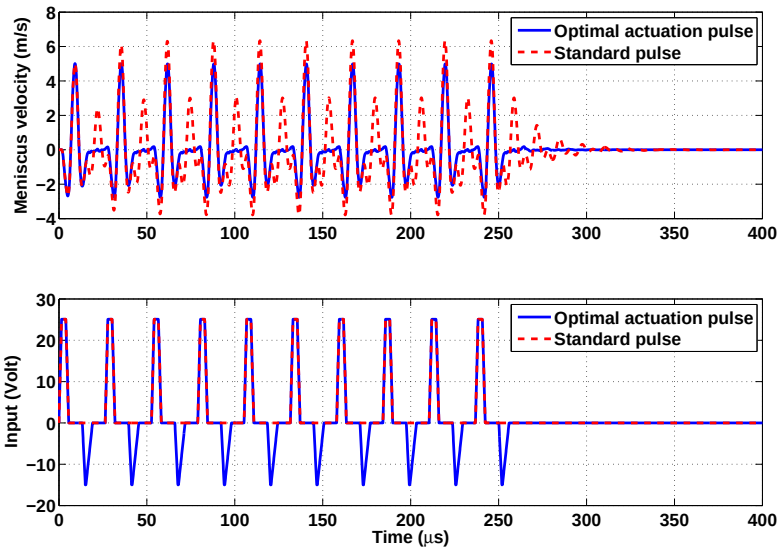

Figure 7: Simulation for jetting of ten drops at DoD frequency 38kHz.

the improvement in the performance of the inkjet printhead. To summarize all the results in Figure 8, we have only plotted the velocity-peak of the tenth drop against the DoD frequency. As the velocity-peak is almost equal to the velocity of the jetted drop, Figure 8 is equivalent to the 'DoD-curve', which is the benchmark defined in the introduction. We have seen previously that the standard pulse is not able to quickly bring the ink channel to a rest. The time allowed for the residual oscillation to settle down will reduce as we increase the DoD frequency. Therefore, as shown in Figure 8, the variation in the peak meniscus velocity becomes larger at higher DoD frequencies when we consider the standard pulse. As opposed to this, the variation of the velocity-peak with the optimal pulse is very limited.

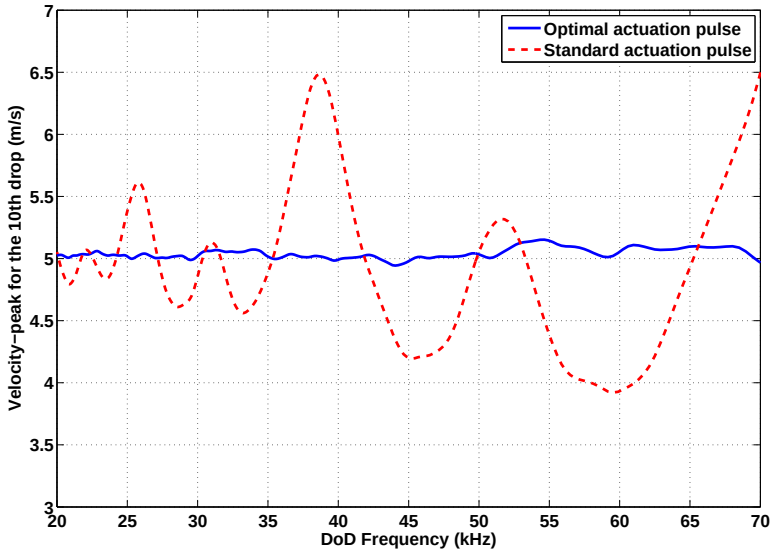

Figure 8: Simulated DoD curve.

Remark:

By adding an extra quenching pulse, the duration of the optimal pulse will always be longer than the standard pulse. The duration of the standard pulse is 5.5 μs while the one of the optimal pulse ($u(k, \theta_{\text{opt}})$) is 19.5 μs. A consequence of the longer duration of the pulse is that, within the range [0 70kHz] for the DoD frequency, the optimal pulses will overlap from a DoD frequency $(1/19.5\,\mu\text{s}) = 51$ kHz. This does not happen for the standard pulse. For $f_{DoD} > 51$ kHz, we have decided to superimpose the overlapping pulses. This means that, if we want to jet a series of N_D drops at a DoD frequency f_{DoD} larger than 51 kHz, we

in fact apply the following voltage $u_{\text{overlap}}(k)$ to the piezo unit

$$u_{\text{overlap}}(k) = \sum_{i=0}^{N_D-1} u_{\text{opt}}\Big(k - i\tau_D\Big)$$

where $u_{\text{opt}}(k) = u(k, \theta_{\text{opt}})$ the optimal pulse of duration $19.5\,\mu$s, and τ_D is the time (expressed in number of samples) between two actuation pulses.[1]

In Figure 5, we observe that the optimal trapezoidal shape allows to reduce significantly the residual oscillations. By considering the approach in Section 3.4, we will now verify whether an even better performance could be achieved if we relax the trapezoidal shape constraint on the actuation pulse. For this purpose, we have solved the least-square problem (7) with a FIR filter $F(q, \beta)$ of length 930 to improve the performance. In Figure 9, we compare the meniscus velocity resulting from the application of the optimal pulse obtained by solving (7) (i.e. the unconstrained pulse) and the meniscus velocity resulting from the application of the optimal pulse obtained by solving (3)-(4) (i.e. the trapezoidal pulse). By analyzing the unconstrained pulse (see the bottom of Figure 9), we must first observe that this unconstrained pulse is very similar to the optimal trapezoidal pulse. The main difference between these two pulses is the oscillating behavior after 15μs in the unconstrained pulse. However, from a practical point of view, the increase of complexity

[1] If T_s is the sampling time and $round(x)$ rounds a real number x to the nearest integer, τ_D is then equal to $round(\frac{1}{T_s f_{\text{DoD}}})$. Indeed, at a DoD frequency of f_{DoD}, the time separating two successive actuation pulses is $\frac{1}{f_{\text{DoD}}}$ second and τ_D must be an integer since $u_{\text{opt}}(k)$ is a discrete-time signal.

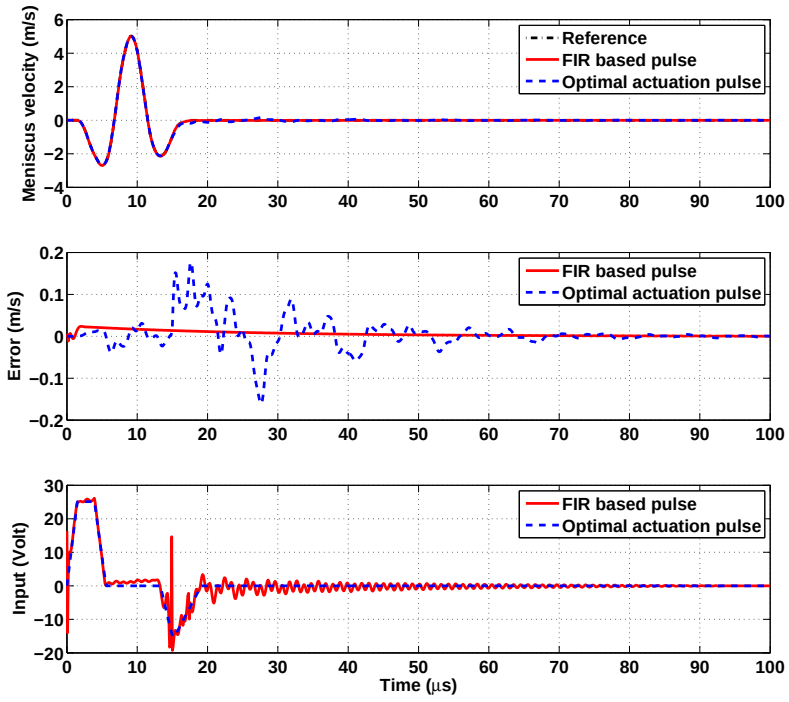

Figure 9: Response of the meniscus velocity to the optimal actuation pulse and the FIR-based actuation pulse.

of the pulse (the oscillatory behavior) outweighs the improvement of performance (the performance with the optimal trapezoidal pulse is already very satisfactory). Considering this, the optimal trapezoidal pulse delivered by the optimization problem (3)-(4) seems the best compromise between performance and complexity. It also indicates that the nonlinear optimization (3)-(4) yields an actuation pulse which is very close to the global optimum.

5. Experimental Results

The simulation results show that significant improvements can be achieved by using the optimal piezo actuation pulse $u(k, \theta_{\text{opt}})$ i.e. the trapezoidal pulse depicted at the bottom of Figure 5. In this section we present experimental results obtained with the optimal actuation pulse $u(k, \theta_{\text{opt}})$, derived in the previous section, to validate this claim. The experimental setup is equipped with a CCD camera which can capture the images of jetted drops at an interval of 10μs. The details about the experimental setup, such as the camera, the microscopic lens etc can be found in [20]. In each experiment we have jetted 10 ink drops from the inkjet channel at a fixed DoD frequency. All the images are placed adjacent to each other in the order of the time instant when they are taken. The composite image constructed in this manner for a DoD frequency equal to 28kHz is shown in Figure 10. This image shows the flight profile of the ten drops from the nozzle to the paper. The vertical axis represents the position of the ink drop. The starting position is the nozzle level and the paper is placed at the end position. The distance between the nozzle and the paper is approximately 2mm. Ideally, it is required that the ten drops should be placed at an equal distance on the paper. In Figure 10,

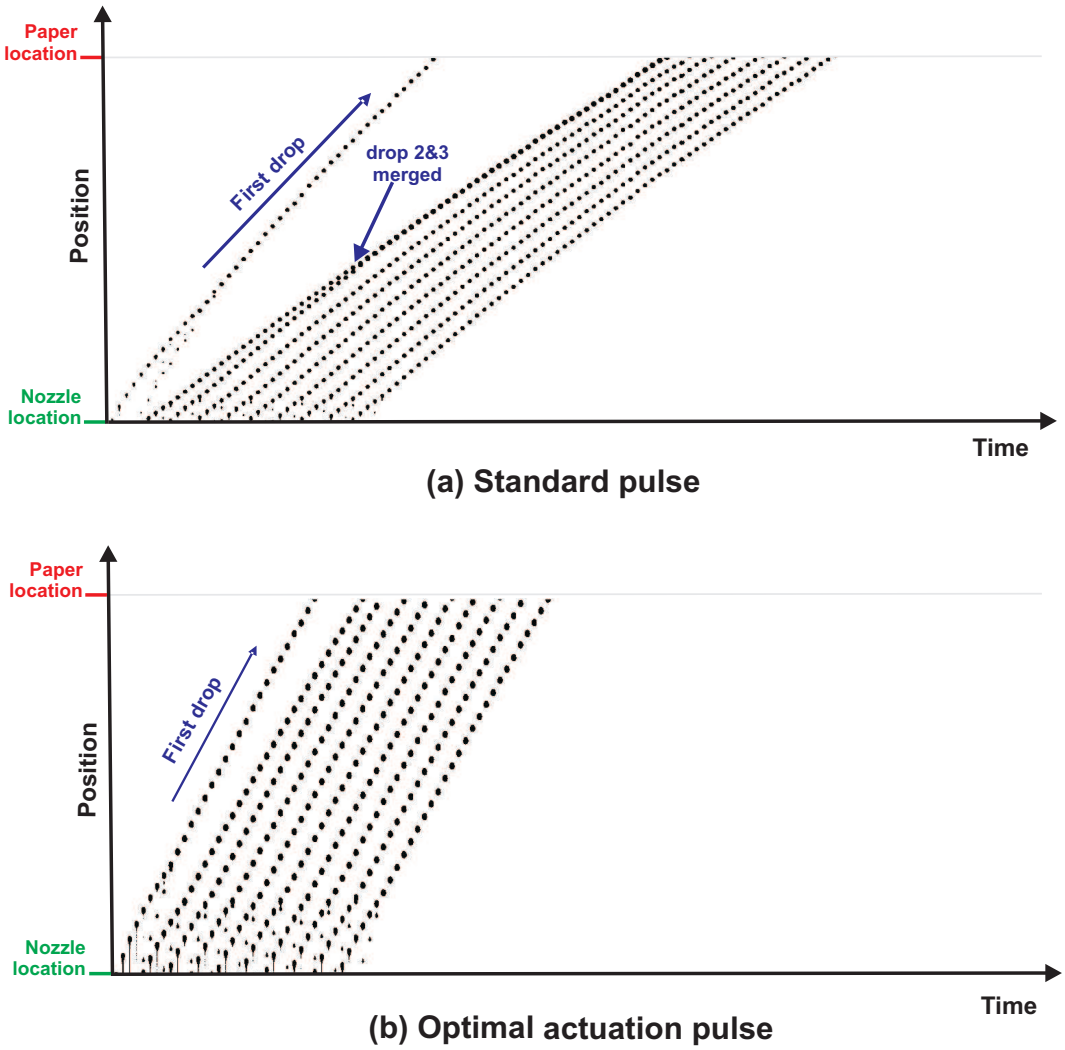

Figure 10: Experimental results: 10 drops jetted at DoD frequency 28kHz.

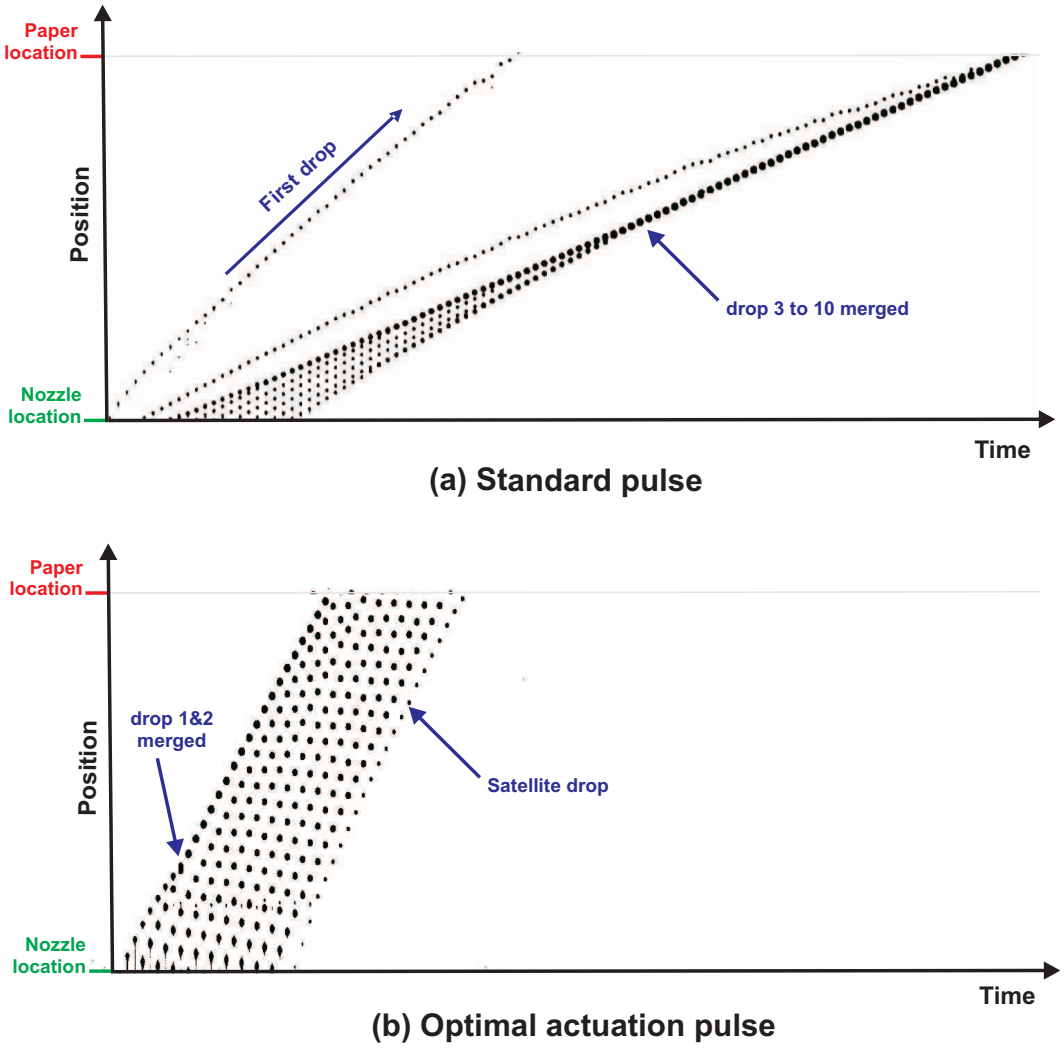

Figure 11: Experimental results: 10 drops jetted at DoD frequency 46kHz.

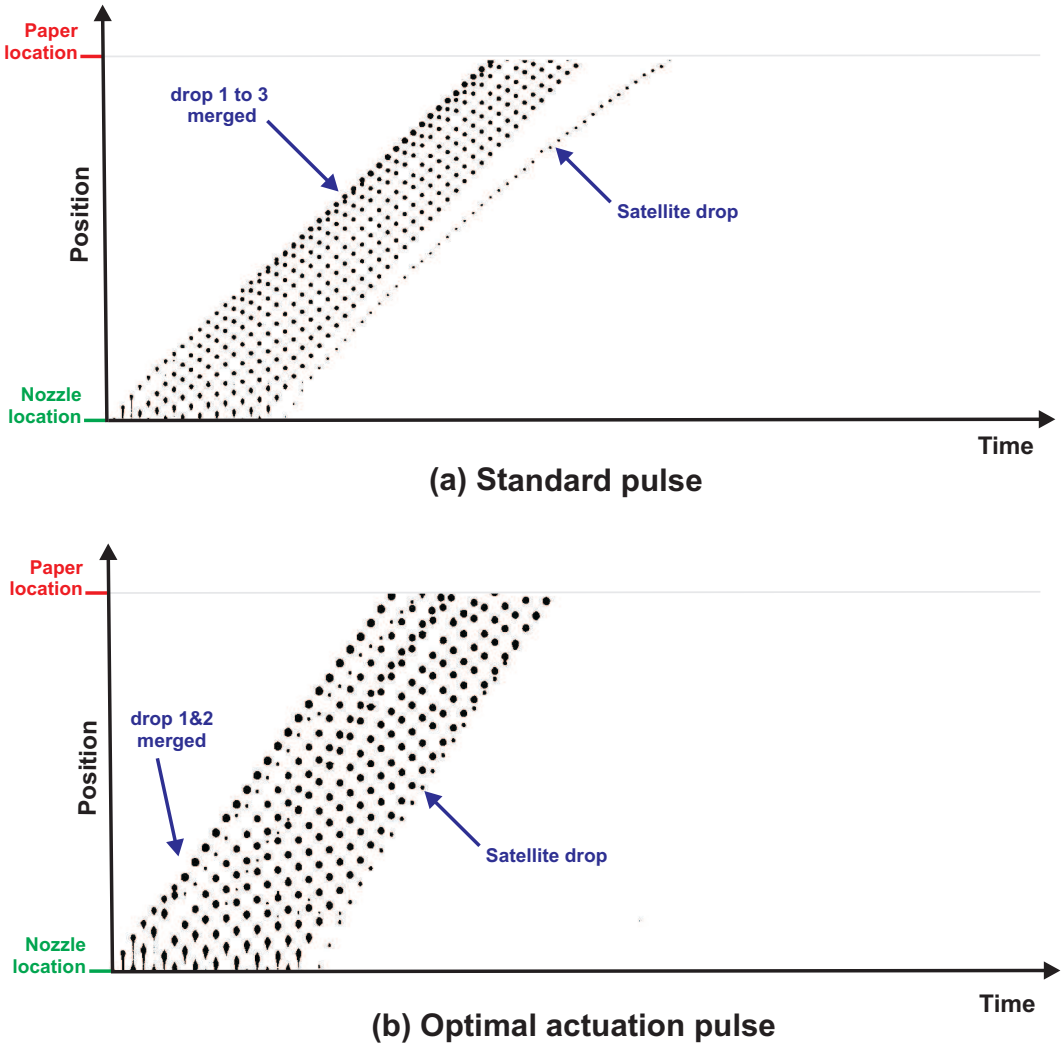

Figure 12: Experimental results: 10 drops jetted at DoD frequency 54kHz.

we compare the result with the standard pulse (Figure 10a) and with the optimal pulse (Figure 10b). Figure 10a shows that, for the standard pulse, the first drop travels to the paper, but the second drop is slower than the first drop and gets merged in the third drop. Only nine drops reach the paper and the first drop is placed far away from the rest of the drops. However, for the optimal pulse, all the ten drops travel with almost the same velocity and they are placed at an equal distance on the paper.

The printhead performance degrades severely when the standard pulse is used at a DoD frequency of 46kHz, shown in Figure 11. Figure 11a shows that for the standard pulse, the first drop travels to the paper. However, the drops jetted subsequently have different velocities and they are slower than the first drop. Therefore, they get merged into a single drop before reaching the paper. Consequently, only two drops eventually reach the paper and they are placed far away from each other. For the optimal actuation pulse, all the jetted drops have almost the same velocity (see Figure 11b). Since they have similar velocities, the drops are placed at an equal distance on the paper. The first drop is however slower and hence caught by the second drop. A small satellite drop is also visible after the tenth drop.

Now let us consider the case of a DoD frequency equal to 54kHz (see Figure 12). In this case, as opposed to the previous cases, the first drop is slower than drops 2, 3 and 4 when the standard pulse is used (see Figure 12a). This has as consequence that the four first drops merge and only seven drops reach the paper. With the optimal pulse, only the two first drops merge. Another advantage of the optimal actuation is that the drops, which do not merge, have similar velocities while these velocities are disparate with

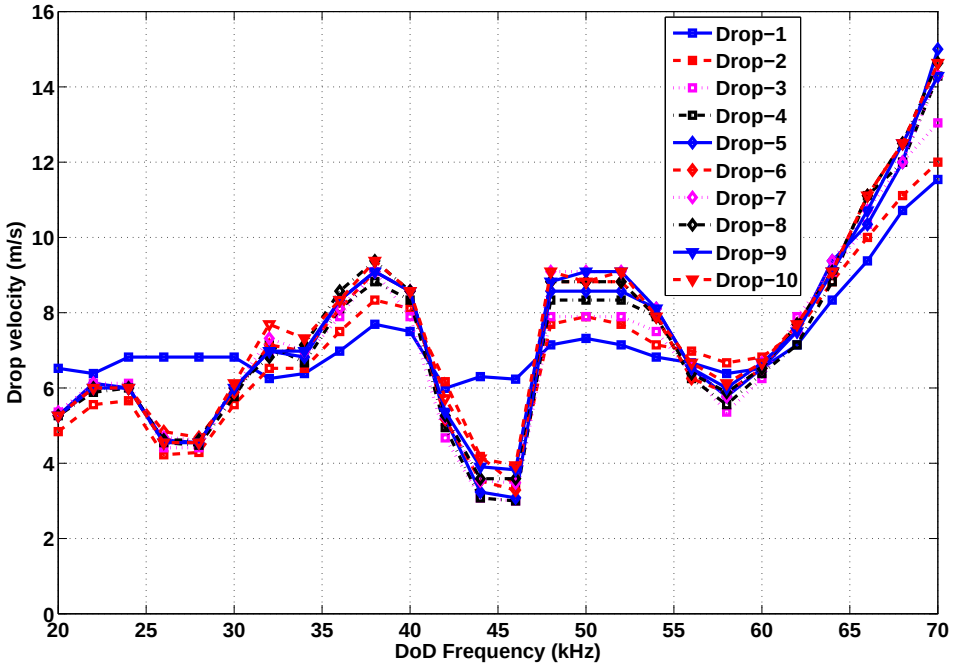

Figure 13: Experimental DoD curve with the standard pulse.

the standard pulse.

Besides the experiments at these 3 DoD frequencies, other experiments were carried out for different DOD frequencies ranging from 20 kHz to 70 kHz with the step of 2 kHz. The drop velocities of each of the 10 drops are shown in Figures 13 and 14 as a function of the DoD frequency (DoD curve). Figure 13 is obtained when the standard pulse is used and Figure 14 shows the results when the optimal pulse is used. As we will show in the sequel, these figures will confirm the observations made for Figures 10-12. We will evaluate the performance observed in these two new figures based on three aspects.

First, we compare the velocity variation of the tenth drop over the DoD frequency range. The velocity of the tenth drop for the standard pulse varies from 5.5ms^{-1} to 14.5ms^{-1}. For the optimal actuation pulse, this variation is considerably smaller: the velocity of the tenth drop varies from 5.5ms^{-1} to 9.8ms^{-1}. Second, at each DoD frequency we look at the velocities of the individual drops. It is very clear that at a fixed DoD frequency, the velocities of the ten drops are quite different for the standard pulse. On the other hand, individual drop velocities are very similar when the optimal pulse is applied to the inkjet printhead. Third, the behavior of the first drop is analyzed over the DoD frequency range. In Figure 13, we observe that, for the standard pulse, the first drop behaves very differently compared to the subsequent nine drops. This can affect the print quality severely, as it appears like a shadow of the printed bitmap to human eyes. When the optimal pulse is used, the difference between the first and the subsequent drops is much less significant. Hence, a bitmap printed with the optimal pulse will not suffer from the shadow effect. The overall improvement in the velocity consistency achieved using the optimal piezo actuation pulse has far-reaching consequences for the print quality. This is because of the proximity of the inkjet printhead to the printing paper. In the simulation results, we observe that the optimal pulse allows us to almost completely remove the residual oscillations. This should imply a flat DoD curve. However, even though we observe significant improvements, the DoD curve is not completely flattened when using the optimal pulse. This could be explained by neglected dynamics. The narrow-gap model cannot predict the meniscus position, it only predicts the meniscus velocity. Once the ink drop is jetted, the ink channel is refilled from the ink

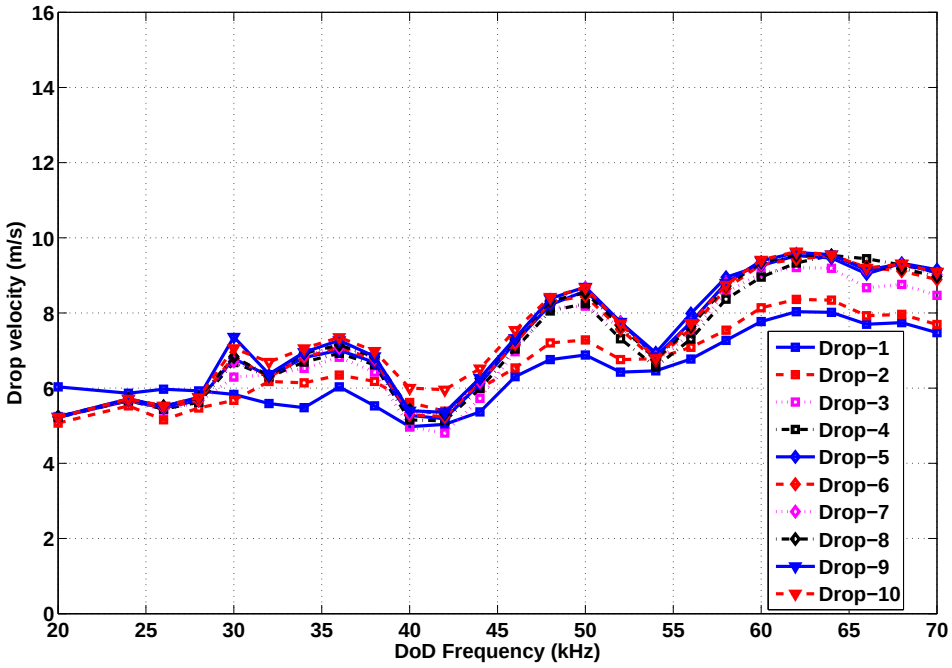

Figure 14: Experimental DoD curve with the optimal actuation pulse.

reservoir. The refill process involves two types of actions, the passive refill and the active refill. In the passive refill, only capillary forces are exerted on the meniscus, whereas in the active refill, oscillations in the meniscus helps to pull the ink from the ink reservoir. In order to achieve ink drops of same properties, it is required to maintain similar initial conditions in the nozzle prior to the application of the actuation pulse. Bringing residual oscillations in the meniscus velocity to zero is not sufficient to bring the meniscus to its initial position and similar initial conditions can therefore not be achieved. Due to this neglected refill dynamics the experimental DoD curve is not completely flat. To handle this issue we are developing a LPV (linear parameter varying) model to describe the ink channel dynamics with the refill effect.

6. Conclusions

In this paper we have proposed an optimization-based feedforward control law to damp the residual oscillations in a DoD inkjet printhead. The simulation results show that the proposed method can very effectively damp the residual oscillations enabling the ink channel to jet ink drops at higher jetting frequencies. Experimental results have demonstrated that considerable improvements in the ink drop consistency can be achieved with the proposed method. The difference between the experimental and the simulation results is attributed to neglected dynamics.

Further improvements can be achieved through a more accurate ink channel model or with an extension of the proposed method to handle parametric uncertainties. This is subject of ongoing research. Applications of the pro-

posed method to multi-channel control will be investigated in the future.

Acknowledgment

This work has been carried out as part of the Octopus project with Océ Technologies B.V. under the responsibility of the Embedded Systems Institute. This project is partially supported by the Netherlands Ministry of Economic Affairs under the Bsik program.

The authors gratefully acknowledge fruitful discussions with W. de Zeeuw, P. Klerken and P. Groenen and technical support from J. Simons.

References

[1] C. Williams. Ink-jet printers go beyond paper. *Physics World*, 19:24–29, 2006.

[2] M.G. Wassink. *Inkjet printhead performance enhancement by feedforward input design based on two-port modeling*. PhD thesis, Delft University of Technology, 2007.

[3] D. B. Bogy and F. E. Talke. Experimental and theoretical study of wave propagation phenomena in drop-on-demand ink jet devices. *IBM J. Res. Dev.*, 28(3):314–321, 1984.

[4] H. Dong, W.W. Carr, and J.F. Morris. An experimental study of drop-on-demand drop formation. *Physics of Fluids*, 18(7):072102, July 2006.

[5] B.W. Jo, A. Lee, K.H. Ahn, and S.J. Lee. Evaluation of jet performance in drop-on-demand (DoD) inkjet printing. *Korean J. Chem. Eng.*, 26(2):339–348, 2009.

[6] K. Kwon and W. Kim. A waveform design method for high-speed inkjet printing based on self-sensing measurement. *Sensors and Actuators A: Physical*, 140(1):75–83, 2007.

[7] H.Y. Gan, X. Shan, T. Eriksson, B.K. Lok, and Y.C. Lam. Reduction of droplet volume by controlling actuating waveforms in inkjet printing for micro-pattern formation. *Journal of Micromechanics and Microengineering*, 19(5):055010, 2009.

[8] MicroFab Technologies Inc. Drive waveform effects on ink-jet device performance. Technical report, 99-03, 1999.

[9] J. Chung, S. Ko, C.P. Grigoropoulos, N.R. Bieri, C. Dockendorf, and D. Poulikakos. Damage-Free low temperature pulsed laser printing of gold nanoinks on polymers. *Journal of Heat Transfer*, 127(7):724–732, July 2005.

[10] K. Kwon. Waveform design methods for piezo inkjet dispensers based on measured meniscus motion. *Journal of Microelectromechanical Systems*, 18 (5):1118–1125., 2009.

[11] H. Wijshoff. *Structure and fluid-dynamics in piezo inkjet printheads*. PhD thesis, University of Twente, 2008.

[12] J.F. Dijksman. Hydrodynamics of small tubular pumps. *Journal of Fluid Mechanics*, 139:173–191, 1984.

[13] M. Ezzeldin, A. Jokic, and P. van den Bosch. Modeling and control of inkjet printhead. In *28th Benelux Meeting on Systems and Control*, Spa, Belgium, 2009.

[14] J.M. Maciejowski. *Predictive control with constraints*. Pearson Education, 2001.

[15] W.M. Beltman. *Viscothermal wave propagation including acoustoelastic interaction*. PhD thesis, University of Twente, 1998.

[16] M.J.D. Powell. A fast algorithm for nonlinearly constrained optimization calculations. In G. A. Watson, editor, *Numerical Analysis*, Lecture Notes in Mathematics, Vol. 630, pages 144–157. Springer Verlag, 1978.

[17] B.N. Pshenichnyj. *The Linearization Method for Constrained Optimization*. Springer-Verlag, Heidelberg, Berlin, Germany, 1994.

[18] J. de Jong. *Air entrapment in piezo inkjet printing*. PhD thesis, University of Twente, 2007.

[19] G.H. Golub and C.F. Van Loan. *Matrix Computations*. John Hopkins Univ. Press, Baltimore, USA, second edition, 1989.

[20] H. Wijshoff. The dynamics of the piezo inkjet printhead operation. *Physics Reports*, 491(4-5):77 – 177, 2010.